

Figure S1. Data processing workflow. Summary of species inclusion across the modeling pipeline for species distributions and viral sharing models. The final analyses in the main text use 3,139 species of placental mammals across all scenarios.

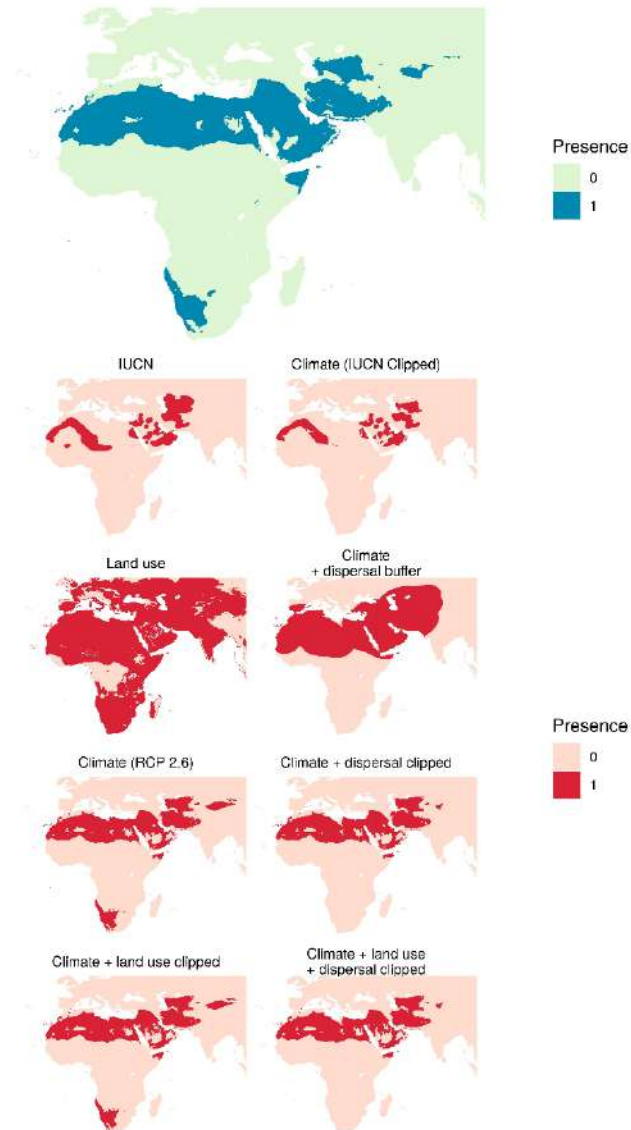


Figure S2. Species distribution modeling workflow for a single species. A focal species (the sand cat, *Felis margarita*) is displayed as an illustrative example. The present day climate prediction (top left) was clipped to the same continent according to the IUCN distribution (top right). This was then clipped according to *Felis margarita*'s land use (second row, left). The known dispersal distance of the sand cat was used to buffer the climate distribution (second row, right). The potential future distribution predictions (RCP 2.6 shown as an example) are displayed in the bottom four panels, for each of the four pipelines: only climate (third row, left); climate + dispersal clip (third row, right); climate + land use clip (bottom row, left) and climate + land use + dispersal clip (bottom row, right). The four distributions clearly display the limiting effect of the dispersal filter (bottom right panels) in reducing the probability of novel species interactions (bottom left panels). The land use clip had little effect on this species as the entire distribution area was habitable for the sand cat.

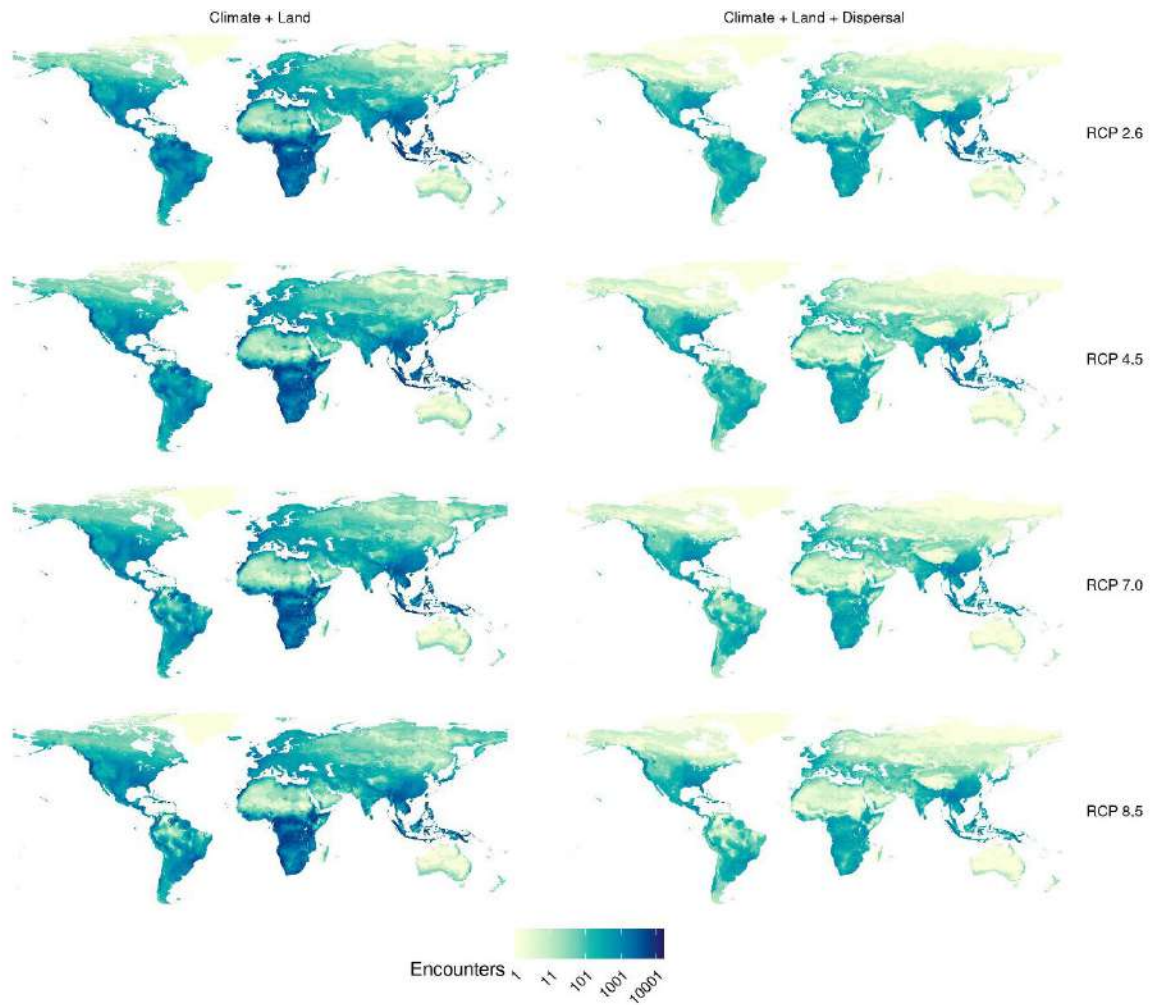


Figure S3. Geographic distribution of first encounters in BCC-CSM2-MR. Predictions were carried out for four representative concentration pathways (RCPs), accounting for climate change and land use change, without (left) and with dispersal limits (right). Darker colours correspond to greater numbers of first encounters in the pixel.

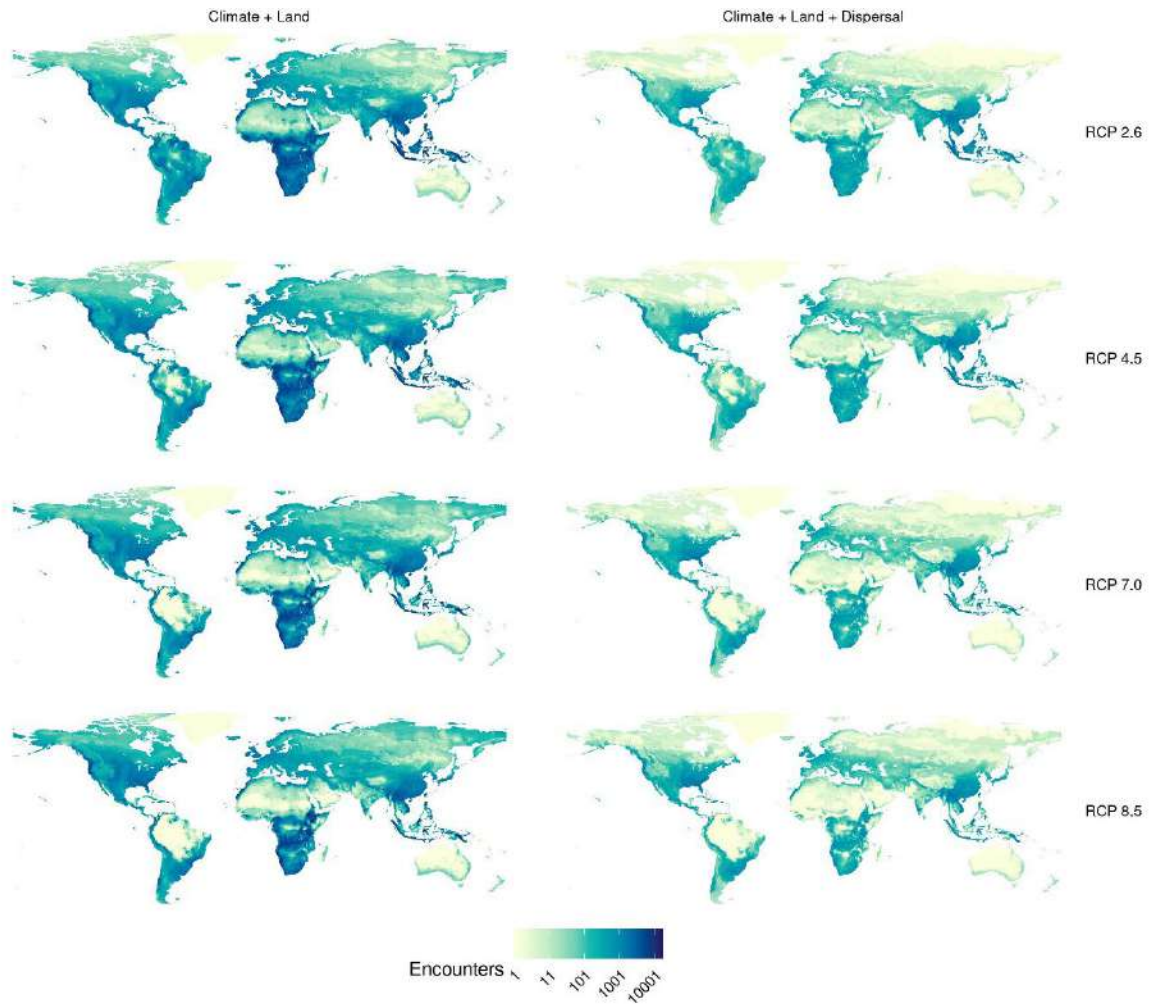


Figure S4. Geographic distribution of first encounters in CanESM5. Predictions were carried out for four representative concentration pathways (RCPs), accounting for climate change and land use change, without (left) and with dispersal limits (right). Darker colours correspond to greater numbers of first encounters in the pixel.

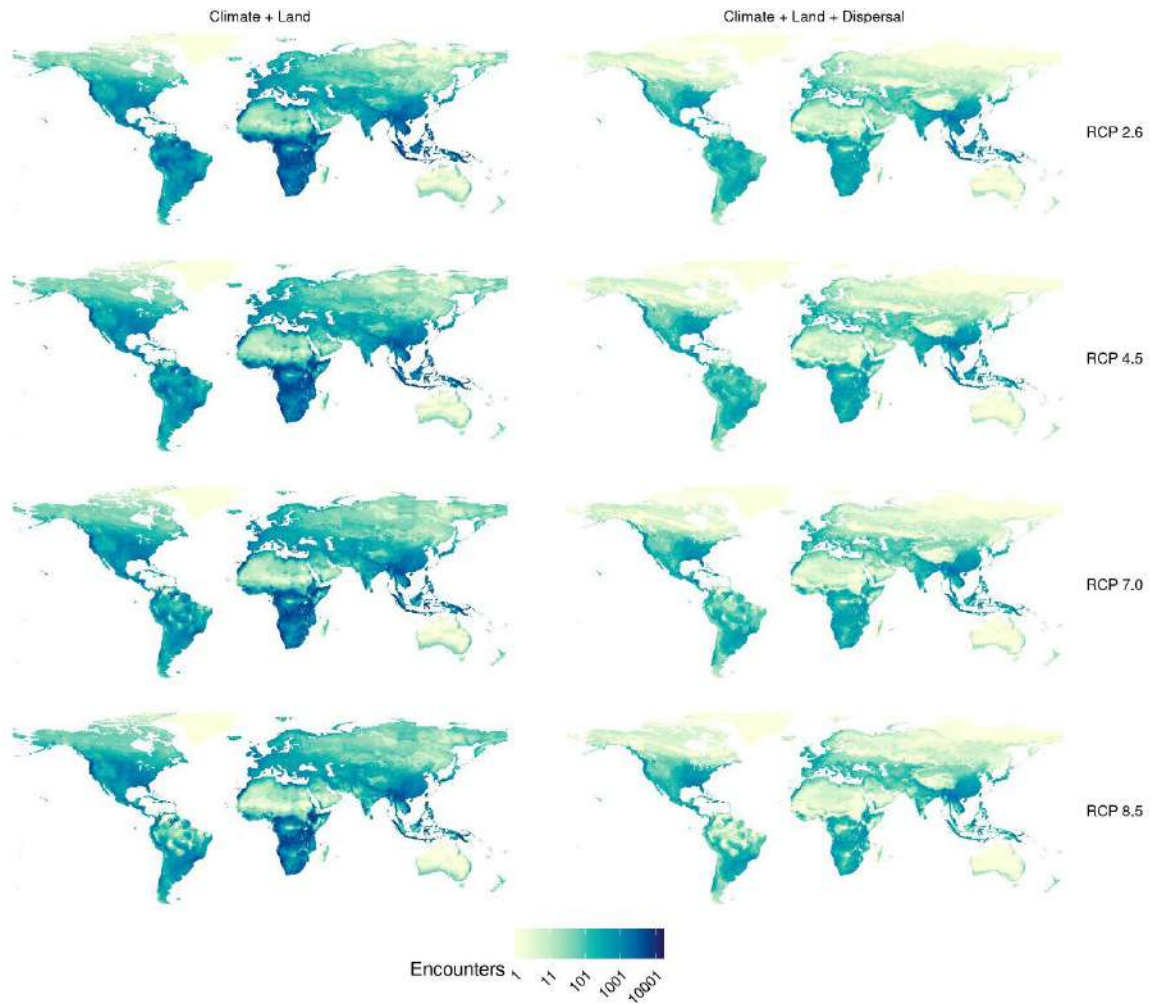


Figure S5. Geographic distribution of first encounters in CNRM-CM6-1. Predictions were carried out for four representative concentration pathways (RCPs), accounting for climate change and land use change, without (left) and with dispersal limits (right). Darker colours correspond to greater numbers of first encounters in the pixel.

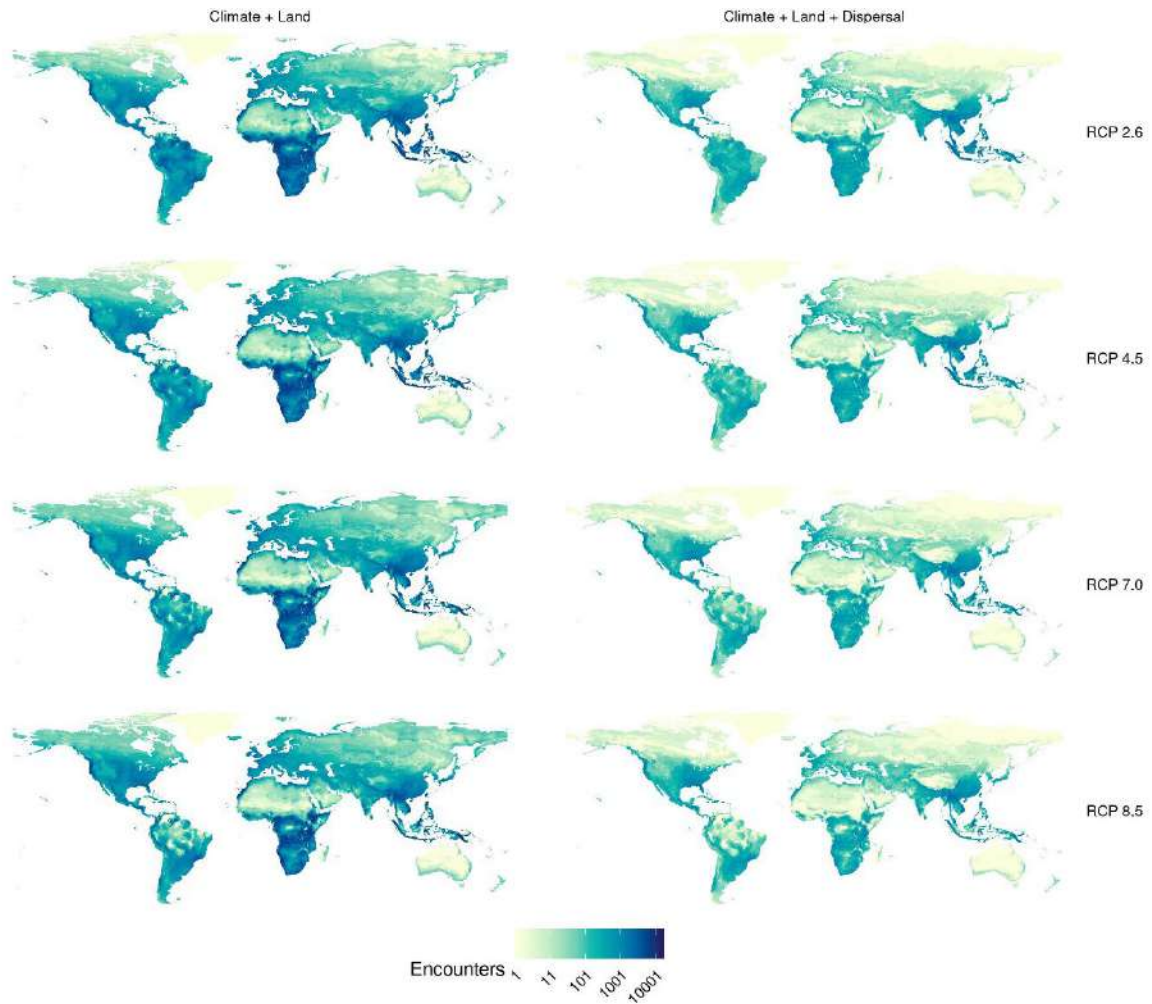


Figure S6. Geographic distribution of first encounters in CNRM-ESM2-1. Predictions were carried out for four representative concentration pathways (RCPs), accounting for climate change and land use change, without (left) and with dispersal limits (right). Darker colours correspond to greater numbers of first encounters in the pixel.

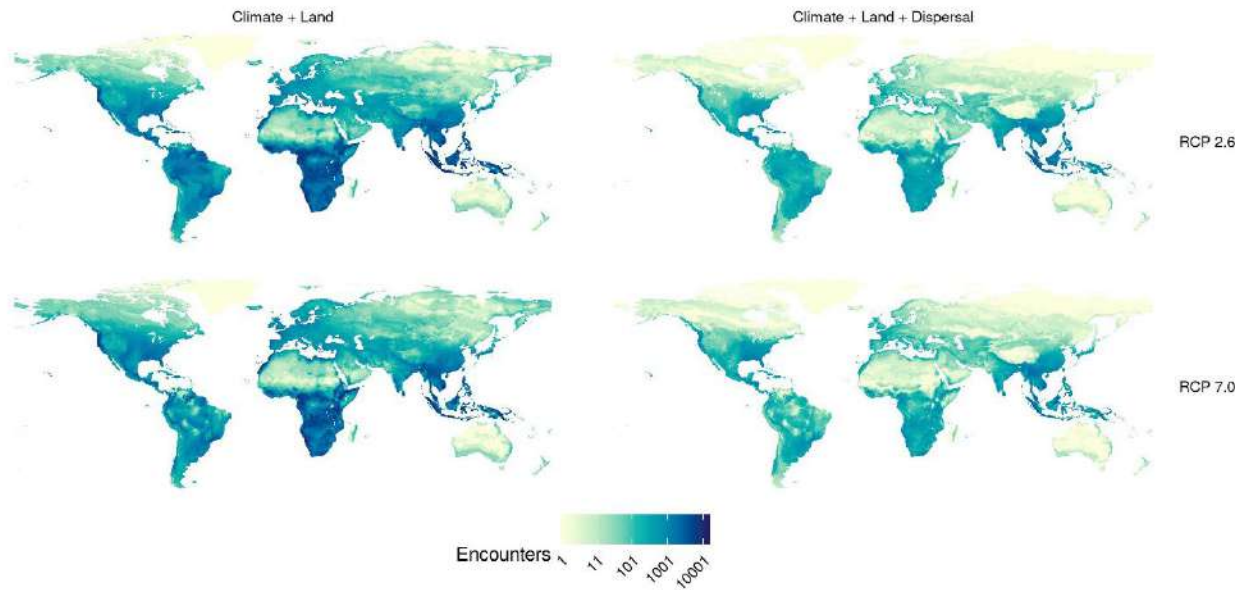


Figure S7. Geographic distribution of first encounters in GFDL-ESM4. Predictions were carried out for the only two available representative concentration pathways (RCPs; see methods), accounting for climate change and land use change, without (left) and with dispersal limits (right). Darker colours correspond to greater numbers of first encounters in the pixel.

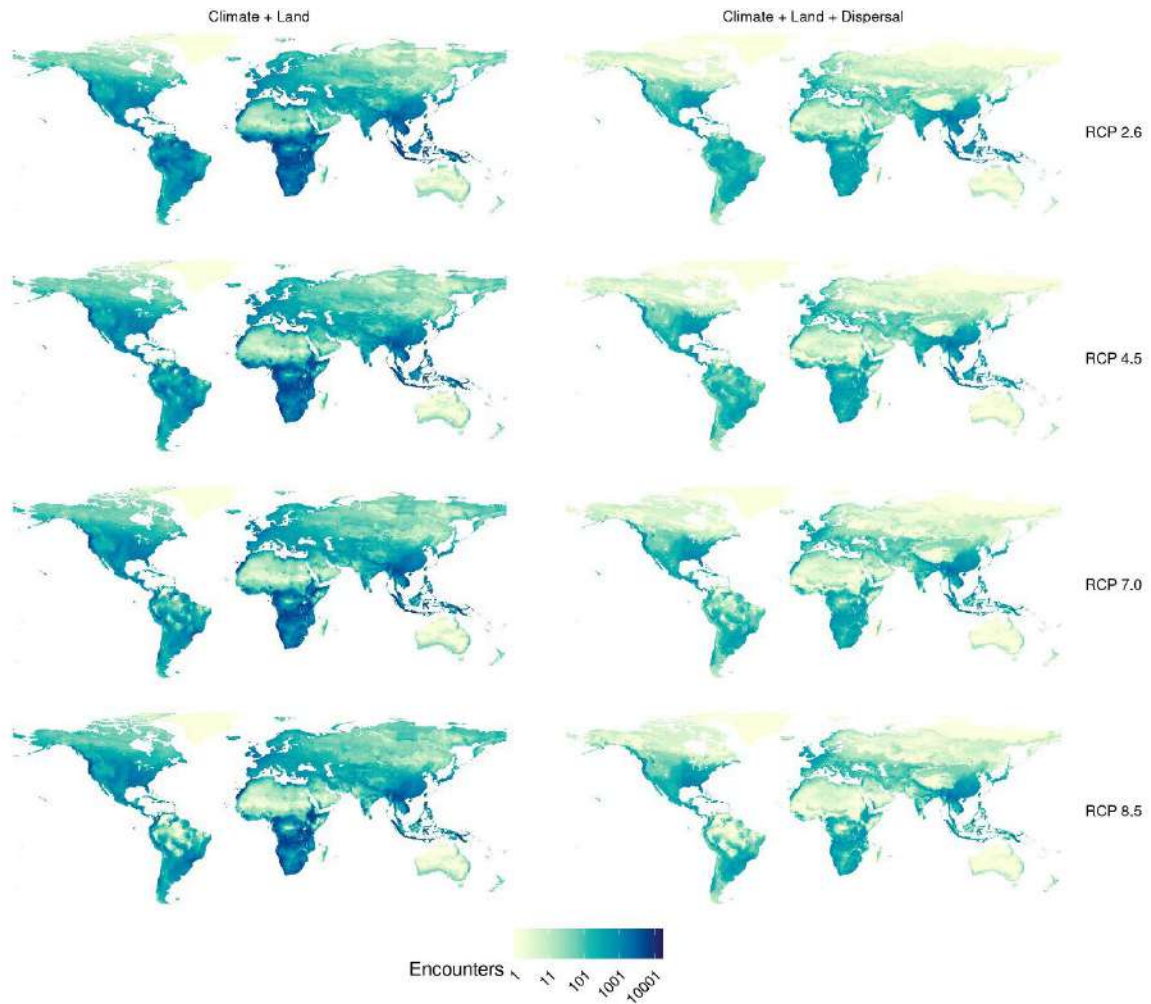


Figure S8. Geographic distribution of first encounters in IPSL-CM6A-LR. Predictions were carried out for four representative concentration pathways (RCPs), accounting for climate change and land use change, without (left) and with dispersal limits (right). Darker colours correspond to greater numbers of first encounters in the pixel.

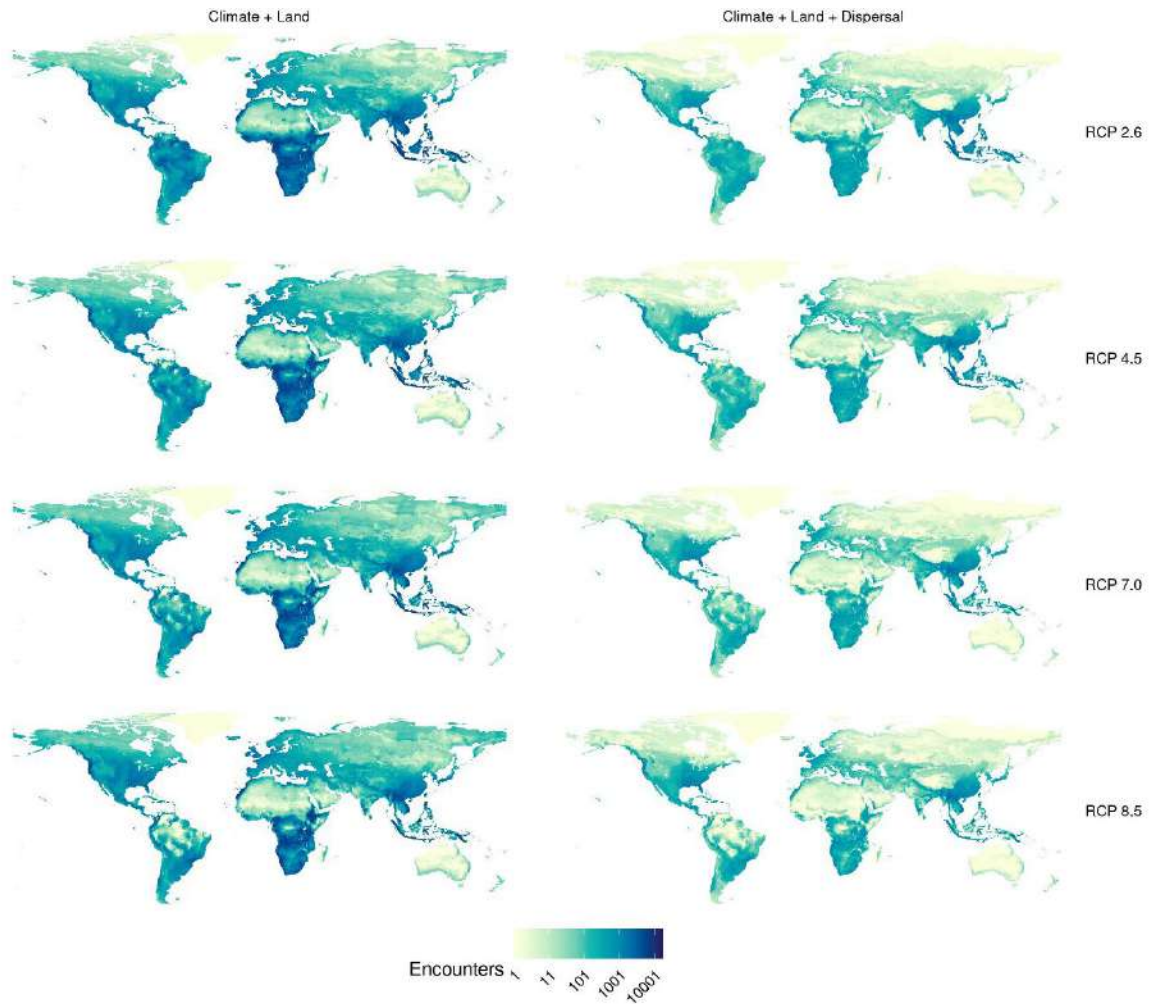


Figure S9. Geographic distribution of first encounters in MIROC-ES2L. Predictions were carried out for four representative concentration pathways (RCPs), accounting for climate change and land use change, without (left) and with dispersal limits (right). Darker colours correspond to greater numbers of first encounters in the pixel.

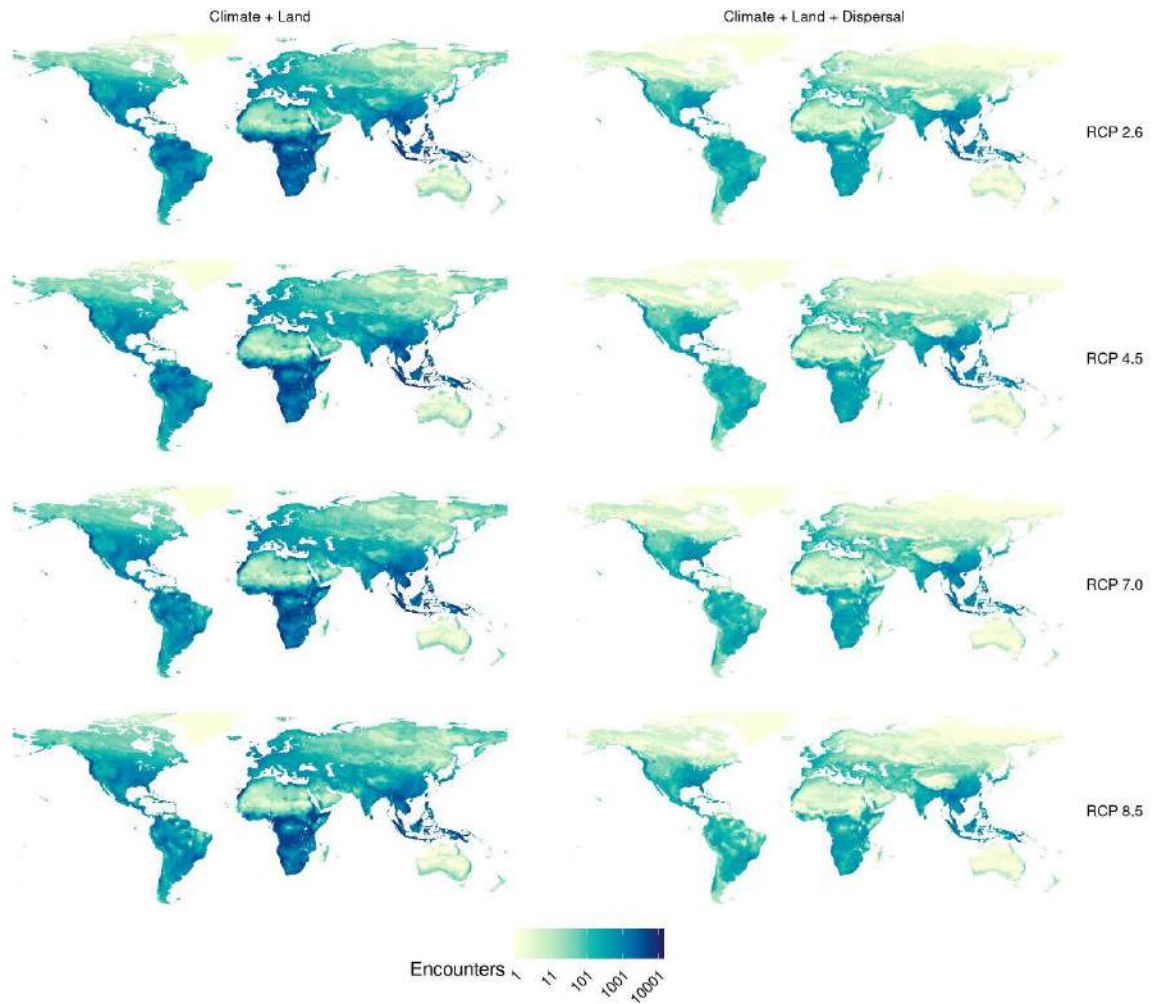


Figure S10. Geographic distribution of first encounters in MIROC6. Predictions were carried out for four representative concentration pathways (RCPs), accounting for climate change and land use change, without (left) and with dispersal limits (right). Darker colours correspond to greater numbers of first encounters in the pixel.

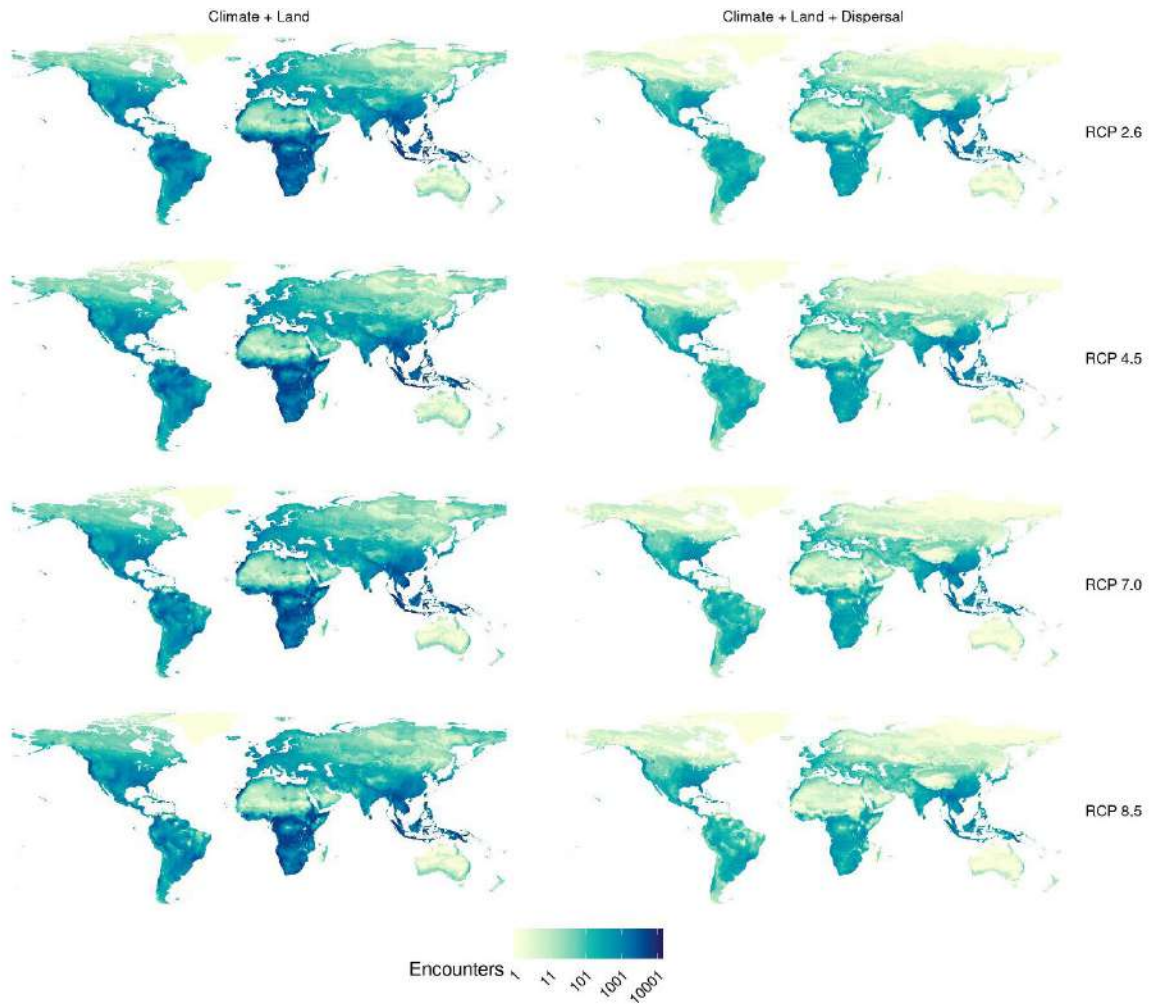


Figure S11. Geographic distribution of first encounters in MRI-ESM2-0. Predictions were carried out for four representative concentration pathways (RCPs), accounting for climate change and land use change, without (left) and with dispersal limits (right). Darker colours correspond to greater numbers of first encounters in the pixel.

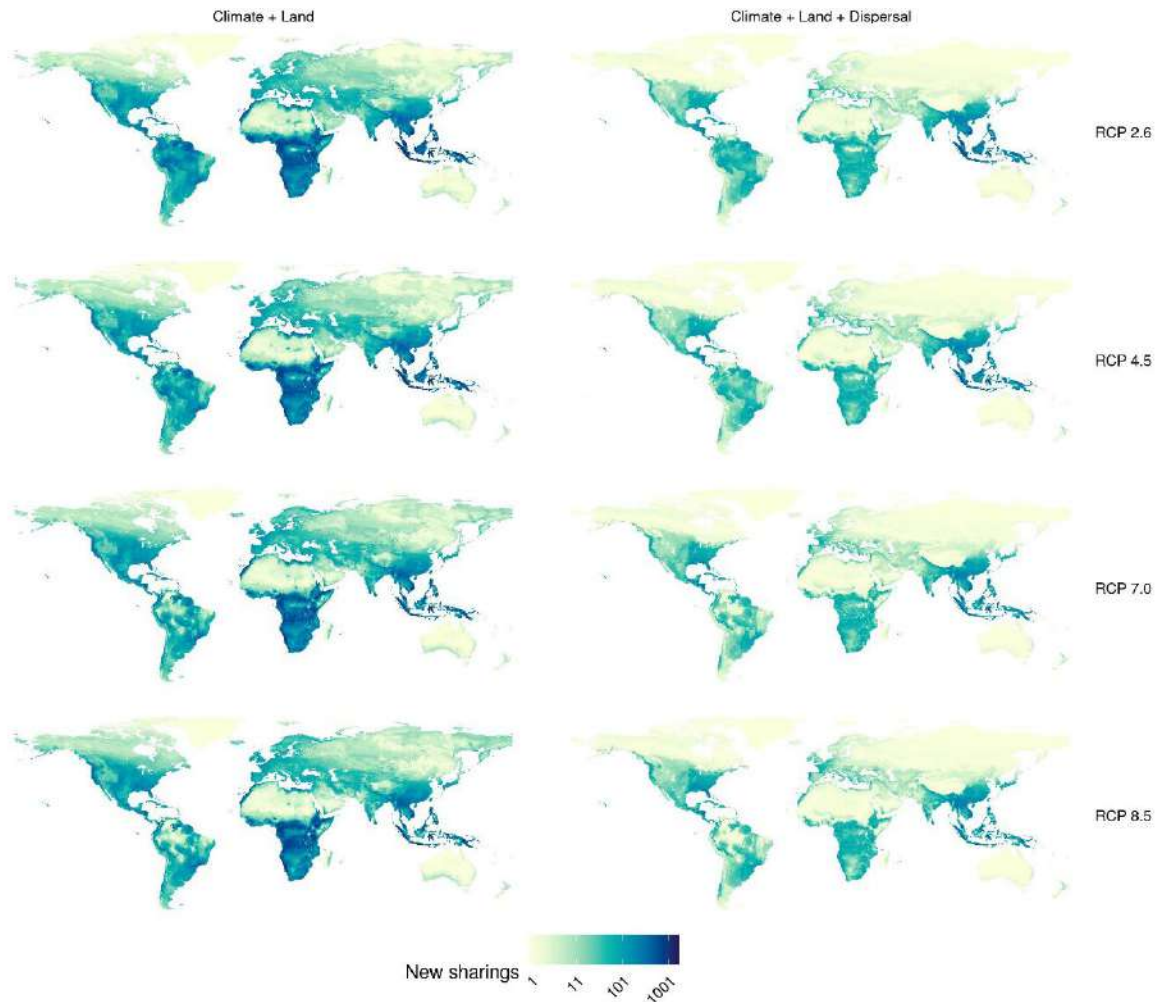


Figure S12. Geographic distribution of viral sharing events in BCC-CSM2-MR. Predictions were carried out for four representative concentration pathways (RCPs), accounting for climate change and land use change, without (left) and with dispersal limits (right). Darker colours correspond to greater numbers of viral sharing events in the pixel.

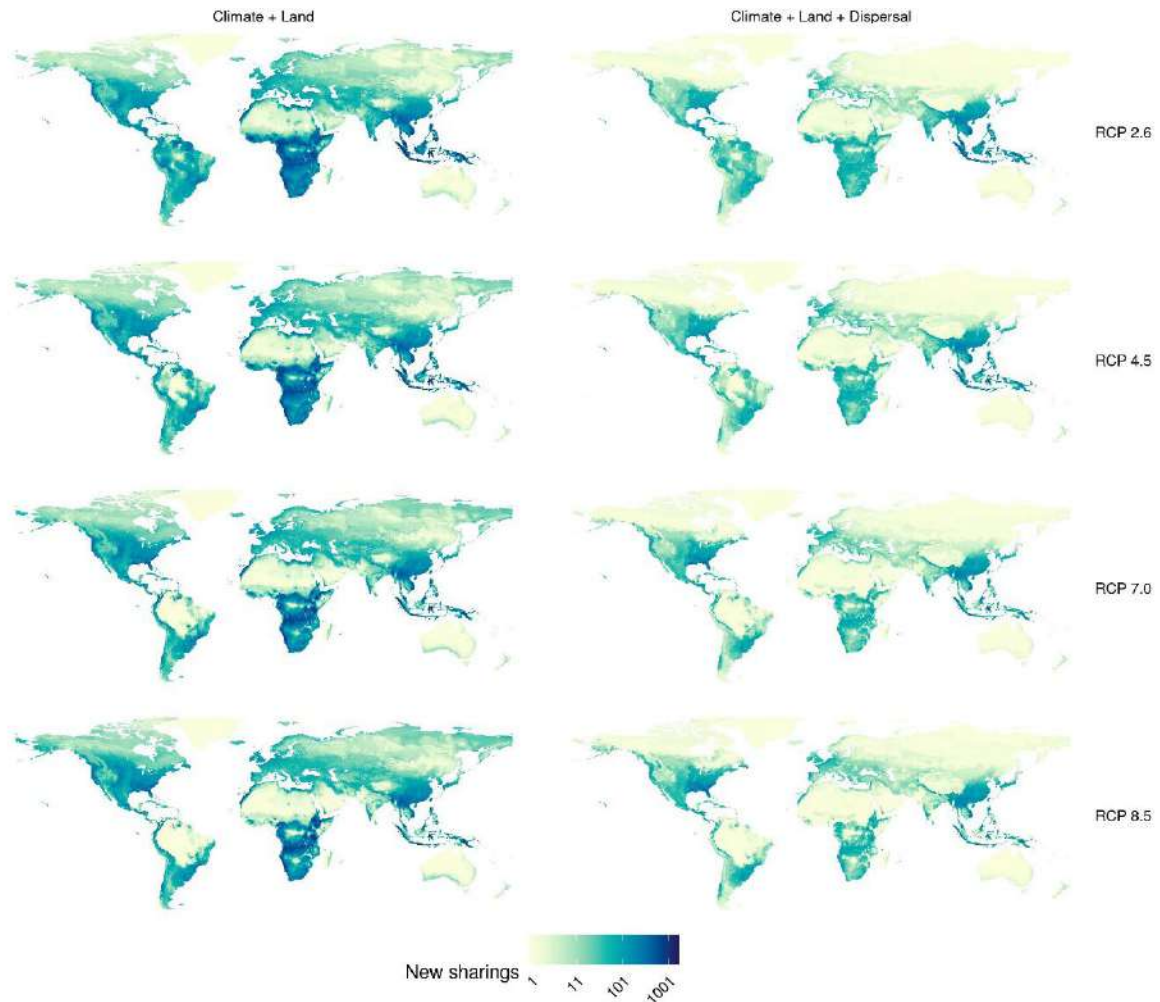


Figure S13. Geographic distribution of viral sharing events in CanESM5. Predictions were carried out for four representative concentration pathways (RCPs), accounting for climate change and land use change, without (left) and with dispersal limits (right). Darker colours correspond to greater numbers of viral sharing events in the pixel.

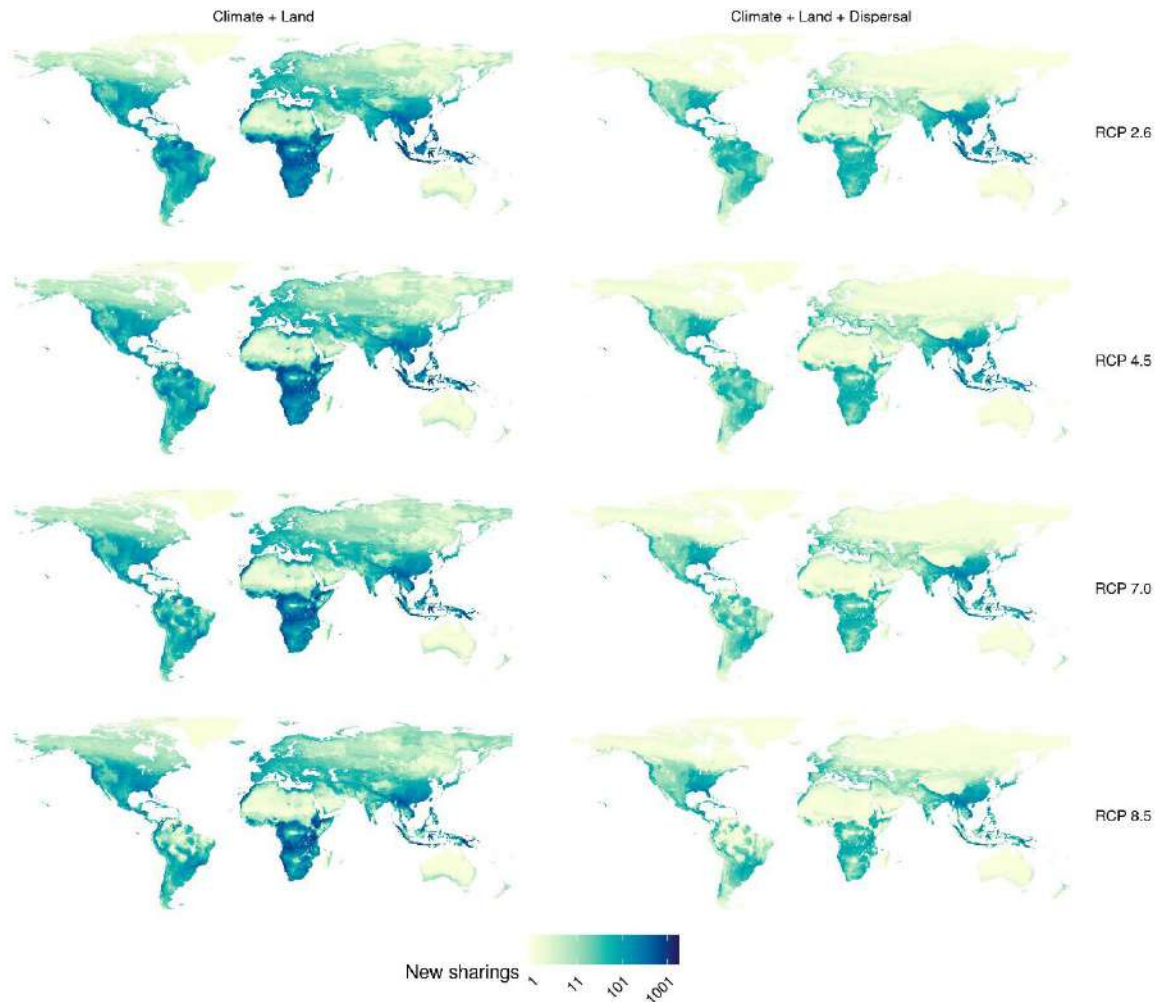


Figure S14. Geographic distribution of viral sharing events in CNRM-CM6-1. Predictions were carried out for four representative concentration pathways (RCPs), accounting for climate change and land use change, without (left) and with dispersal limits (right). Darker colours correspond to greater numbers of viral sharing events in the pixel.

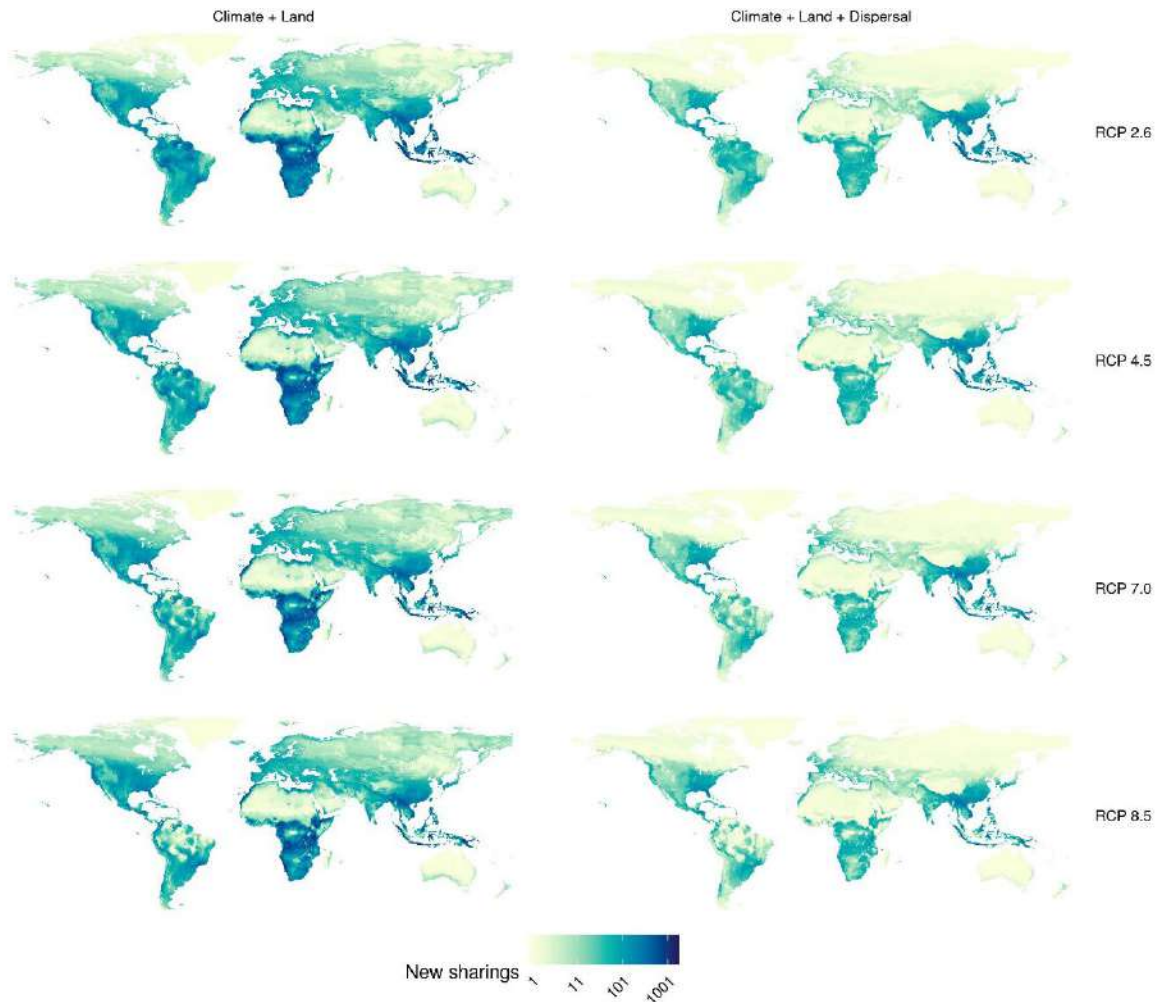


Figure S15. Geographic distribution of viral sharing events in CNRM-ESM2-1. Predictions were carried out for four representative concentration pathways (RCPs), accounting for climate change and land use change, without (left) and with dispersal limits (right). Darker colours correspond to greater numbers of viral sharing events in the pixel.

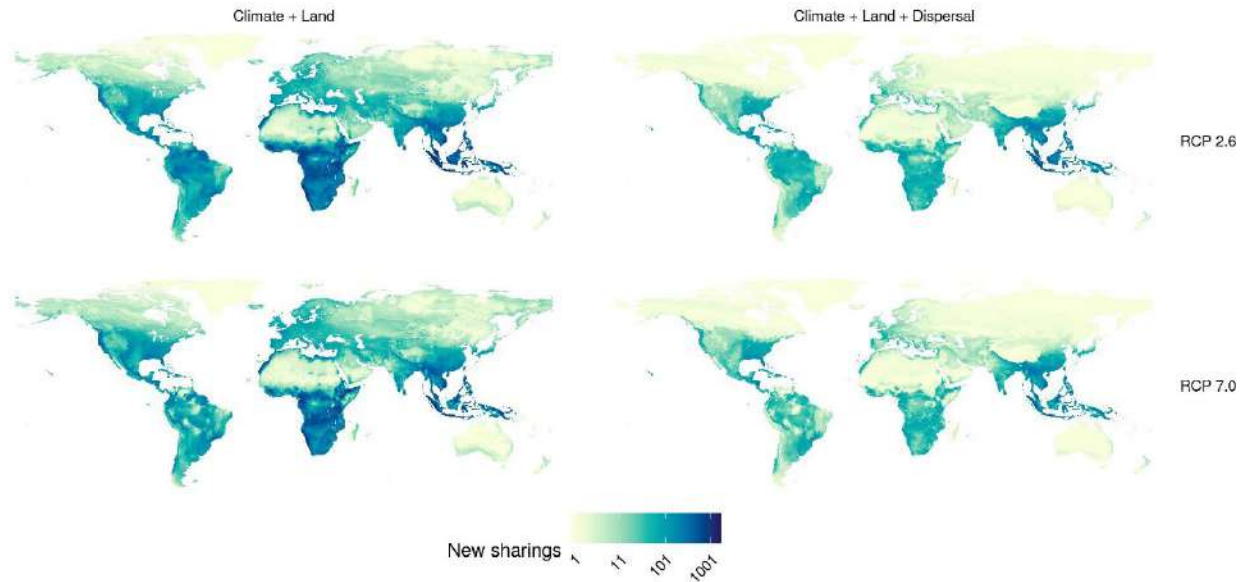


Figure S16. Geographic distribution of viral sharing events in GFDL-ESM4. Predictions were carried out for the only two available representative concentration pathways (RCPs; see methods), accounting for climate change and land use change, without (left) and with dispersal limits (right). Darker colours correspond to greater numbers of viral sharing events in the pixel.

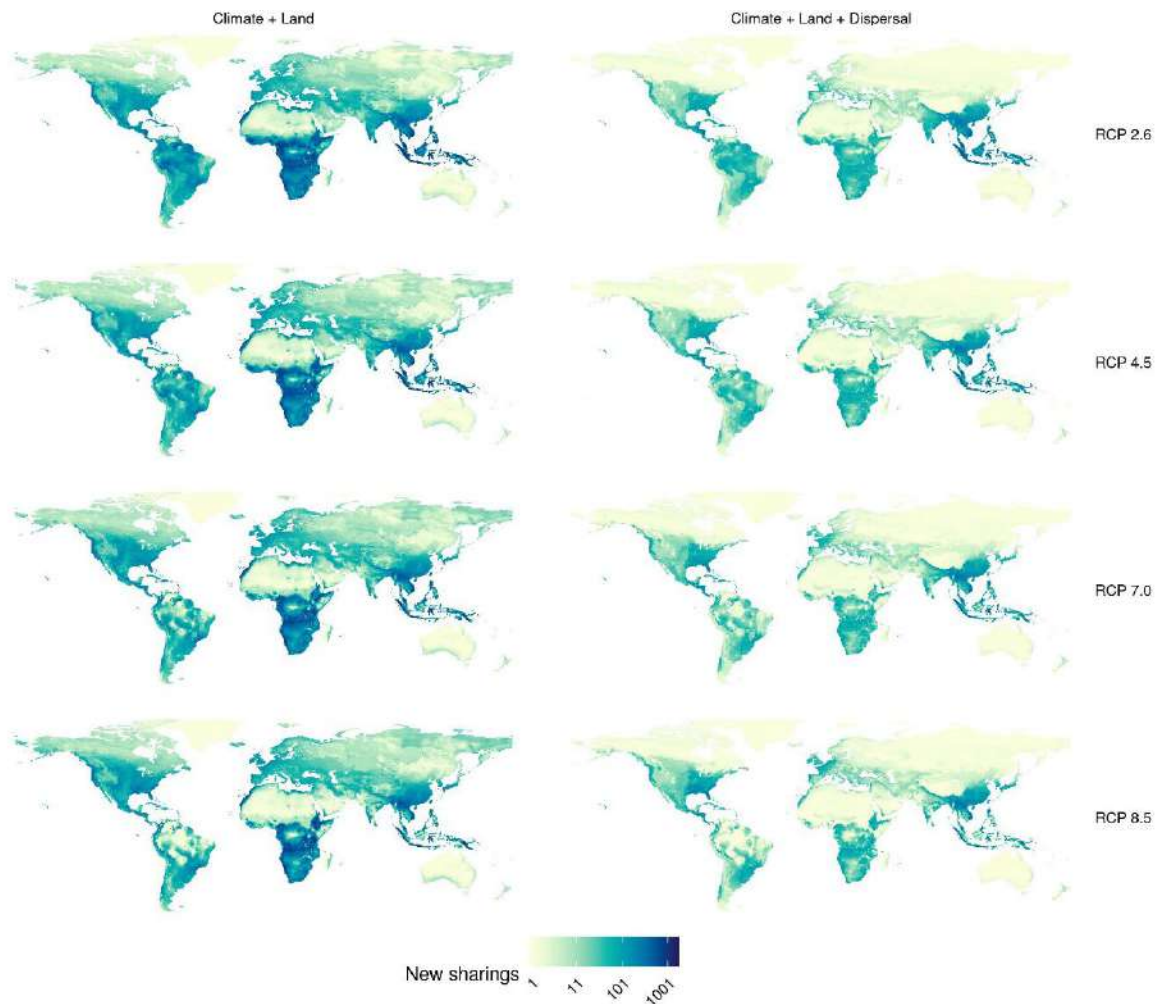


Figure S17. Geographic distribution of viral sharing events in IPSL-CM6A-LR. Predictions were carried out for four representative concentration pathways (RCPs), accounting for climate change and land use change, without (left) and with dispersal limits (right). Darker colours correspond to greater numbers of viral sharing events in the pixel.

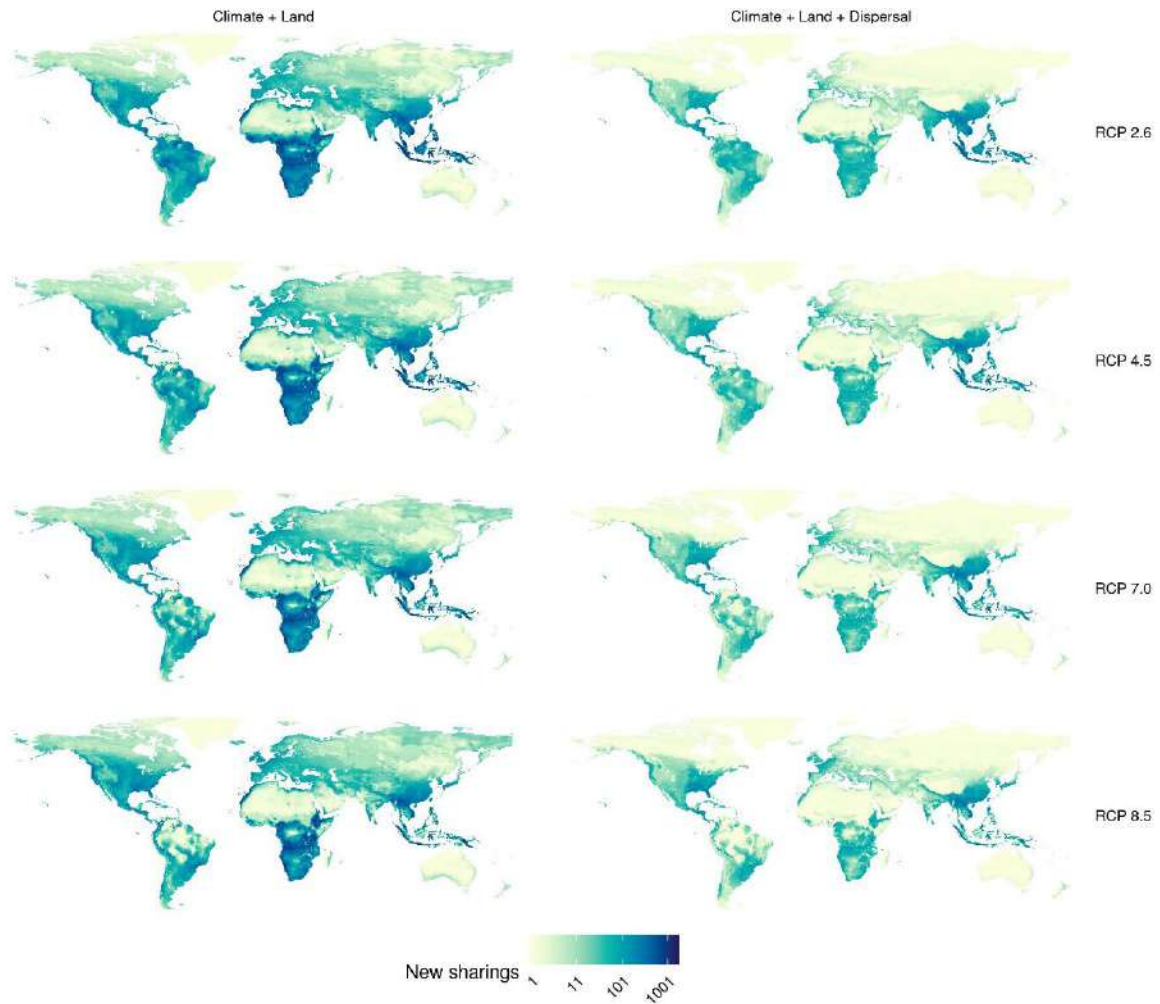


Figure S18. Geographic distribution of viral sharing events in MIROC-ES2L. Predictions were carried out for four representative concentration pathways (RCPs), accounting for climate change and land use change, without (left) and with dispersal limits (right). Darker colours correspond to greater numbers of viral sharing events in the pixel.

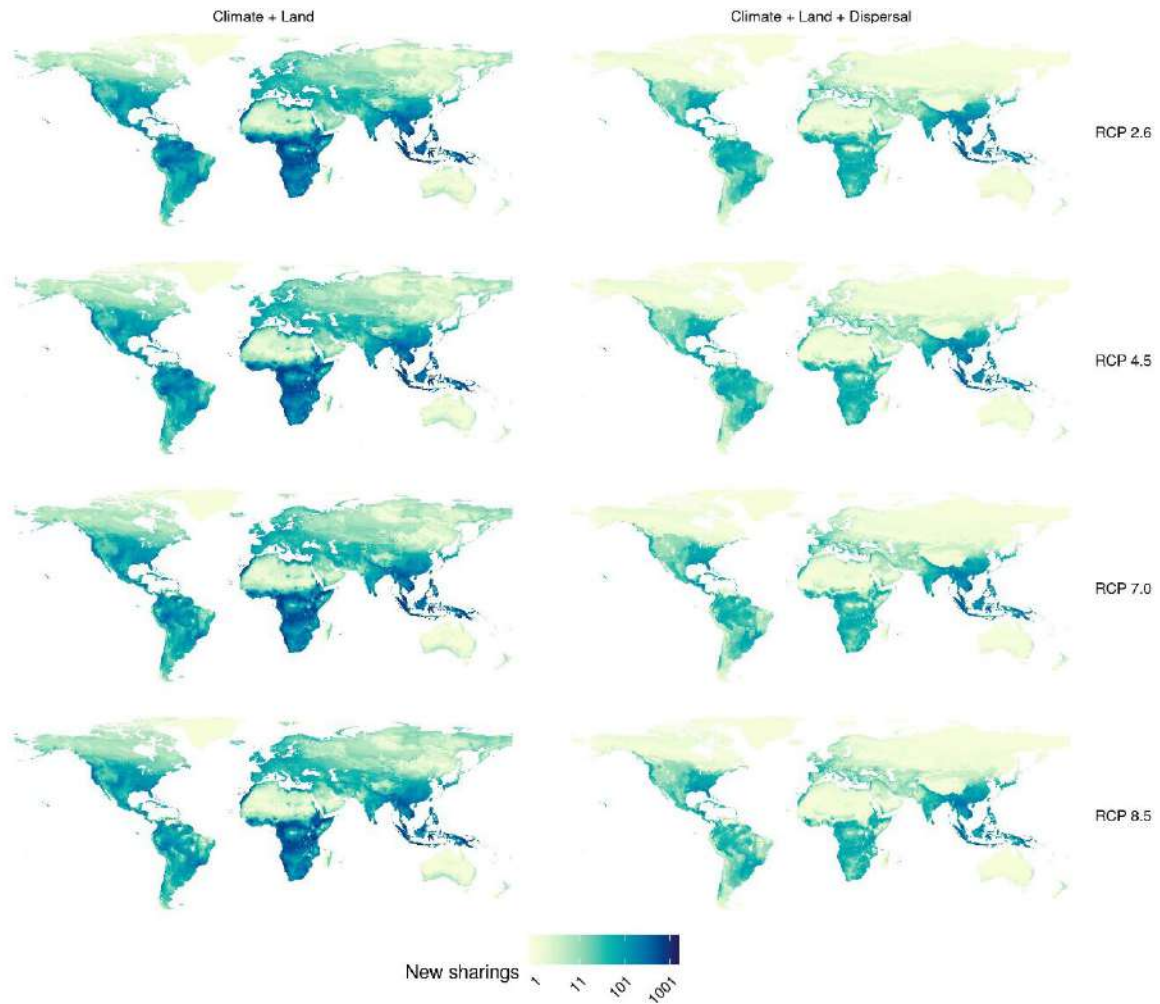


Figure S19. Geographic distribution of viral sharing events in MIROC6. Predictions were carried out for four representative concentration pathways (RCPs), accounting for climate change and land use change, without (left) and with dispersal limits (right). Darker colours correspond to greater numbers of viral sharing events in the pixel.

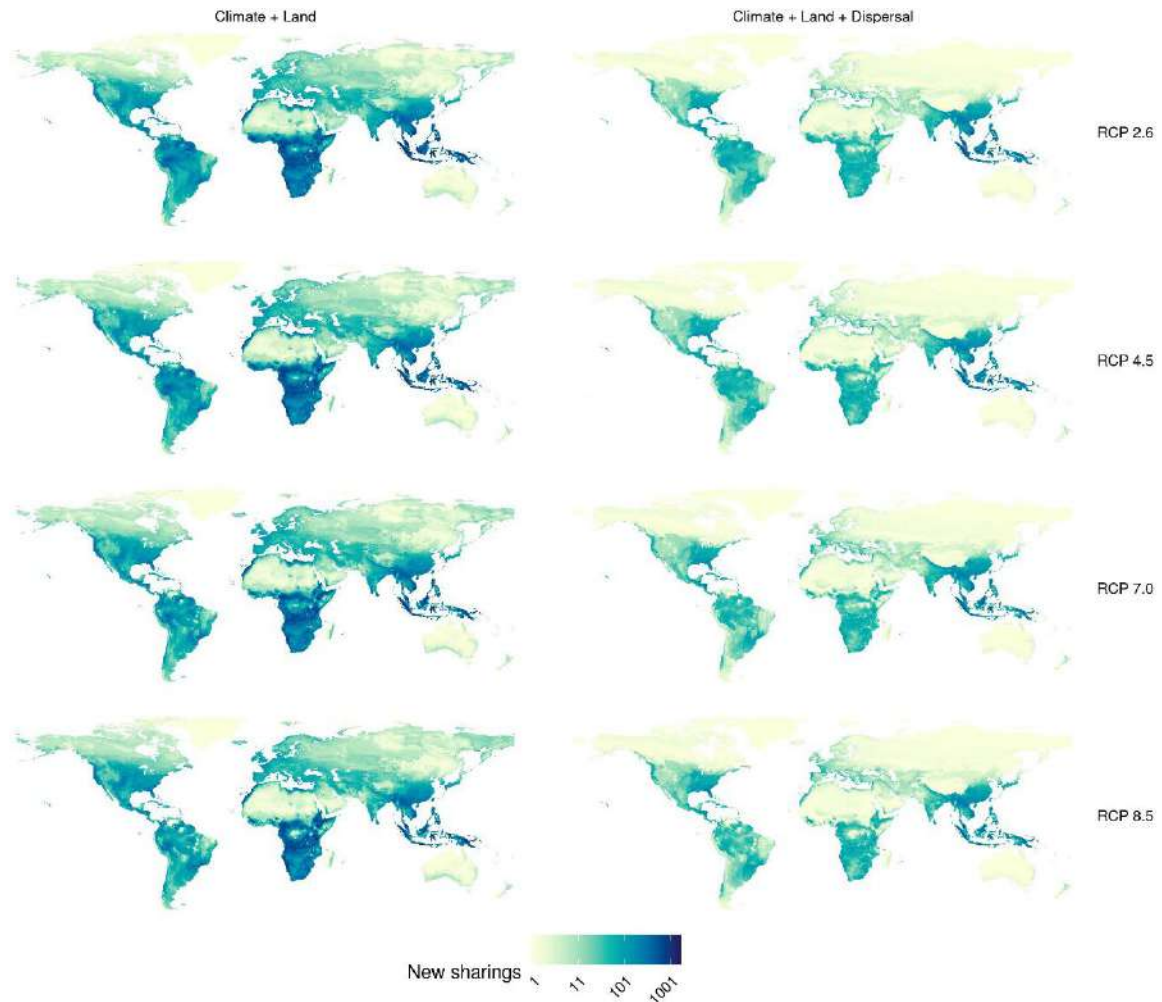


Figure S20. Geographic distribution of viral sharing events in MRI-ESM2-0. Predictions were carried out for four representative concentration pathways (RCPs), accounting for climate change and land use change, without (left) and with dispersal limits (right). Darker colours correspond to greater numbers of viral sharing events in the pixel.